New Magnetite Nanoparticles Enhance Magnetic Resonance Imaging

Biologically friendly and effectively magnetic nanoparticles are crucial for magnetic resonance imaging in biomedical applications. Novel magnetic nanoparticles, Gd^{3+}-chelated Fe_3O_4@SiO_2, were synthesized in buildup of mesoporous shell over magnetite particle surface with Gd^{3+} ions immobilized inside the confined channels. With biologically friendly property, the novel nanoparticles possess transverse relaxivity 681 $s^{-1}mM^{-1}$, 7-fold higher than bare magnetite's. Therefore, the nanoparticles have effectively enhanced magnetic resonance imaging and clearly imaged lymph nodes.

C.-S. Yeh
National Cheng Kung University, Taiwan

C.-C. Huang
National Yang Ming University, Taiwan

U. Jeng
NSRRC, Taiwan

Fe_3O_4 (magnetite) nanoparticles are relatively friendly to the biological system and have been common magnetic materials in numerous biomedical applications. Unfortunately, Fe_3O_4 nanoparticles have less saturation magnetization (Ms), resulting in limited r_2 relaxivity, due to their oxidized states as compared with other magnetic nanoparticles. As a consequence, using higher magnetization nanomaterials, such as bimetallic ferrite nanoparticles, e.g. $MnFe_2O_4$, $CoFe_2O_4$, have been the alternative choice. However, the additional transition metal ions other than iron as contrast agent have always been a concern for their deleterious effect on physiological circumstance. Herein, we have demonstrated that buildup of mesoporous shell over magnetite particle surface with Gd^{3+} ions immobilized inside the confined channels is able to significantly enhance r_2 relaxivity for Fe_3O_4 nanoparticles.[1]

Magnetite nanoparticles were prepared using a thermal decomposition reaction of iron acetylacetonate, Fe(acac) 3, plus oleic acid and trioctylamine. Figure 1(a) shows a high-resolution synchrotron X-ray powder diffraction of as-obtained iron oxide nanoparticles with the diffraction peaks of the crystalline cubic inverse spinel of bulk Fe_3O_4. Magnetite exhibits a strong band at approximately 670 cm^{-1}, assigned as the A_{1g} mode, accompanied with a weak transition near 540 cm^{-1} due to the T_{2g} mode (Fig. 1(b)). A TEM image (Fig. 1(c)) reveals Fe_3O_4 nanoparticles with an edge length of ~ 22 nm. The nanoparticles had the shape of a truncated octahedron. Notably, the (110) reflection of α-Fe appeared in the magnetite. Rietveld refinement showed that the Fe_3O_4 particles contained 7.51% α-Fe (Fig. 1(a)). Figure 1(d) shows the zero field cooling (ZFC) and field cooling (FC) magnetization measurements (M-T curves) at 100Oe. A sharp feature appeared at 120K, corresponding to the signature of the Verwey transition temperature (T_V), an indicator of chemical purity in magnetite. Thus, our synthesis of 22 nm sized Fe_3O_4 nanoparticles can be viewed with satisfactory stoichiometry in the formation of magnetite.

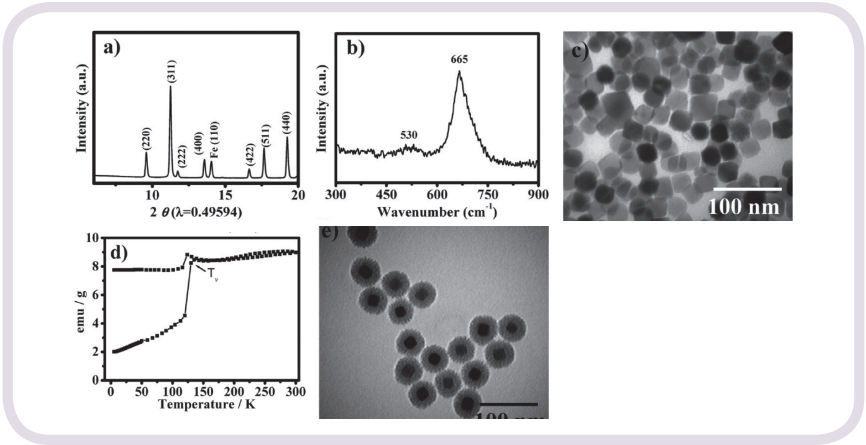

Fig. 1: (a) XRD spectrum using a high-resolution synchrotron X-ray (λ = 0.49594 Å) source, (b) Raman spectrum, (c) TEM image, and (d) ZFC-FC curve for Fe_3O_4 nanoparticles. (e) TEM image for Fe_3O_4 @SiO_2 nanoparticles.

The as-prepared magnetic nanoparticles were surface-modified with CTAB surfactants, and then the Fe_3O_4@CTAB nanoparticles were further accessed using hydrolysis condensation of the TEOS molecules forming the mesoporous silica shell around

the nanoparticles. The Fe_3O_4@SiO_2 nanoparticles (Fig. 1(e)) were composed of 18-nm thick silica shells with pores in the range of 2-4 nm measured from high-magnification TEM images.

The small-angle X-ray scattering (SAXS) data measured for the water solutions containing Fe_3O_4@SiO_2 nanoparticles (after APTES treatment) and the Gd^{3+}-chelated Fe_3O_4@SiO_2 nanoparticles infiltrated the pores of the SiO_2 shell. With Gd^{3+} ions adsorbed into the pores of the SiO_2 shell, giving it increased electron density, the Gd^{3+} chelated Fe_3O_4@SiO_2 nanoparticles exhibit a stronger scattering, especially in the lower Q region (< 0.1 $Å^{-1}$) dominated by the global core-shell structure. In the higher Q region, > 0.12 $Å^{-1}$, the scattering is dominated by small nanopores or is filled with Gd^{3+} ions. A model of polydispersed core-shell spheres for the large Fe_3O_4@SiO_2 nanoparticles, together with an ellipsoid model for small nanopores in the SiO_2 shell, fits the data well. The structural parameters obtained from the SAXS analysis are consistent with those observed using the corresponding TEM images and BJH analysis. For comparison, without nanopores in the SiO_2 shell, well-overlapped SAXS profiles for the Fe_3O_4@SiO_2 nanoparticles (CTAB surfactants had not been removed: "without nanpores") in a pure water solution and a similar solution with Gd^{3+} ions indicate no Gd^{3+} adsorption to the nanoparticles with no nanopores because there was CTAB inside the pores preventing the Gd^{3+} from entering. "Fe_3O_4@SiO_2 (without nanopores) + Gd^{3+} " indicates that Fe_3O_4@SiO_2 nanoparticles with CTAB surfactants were physically mixed with Gd^{3+} ions using $GdCl_3$.[1]

To access the relaxation rate and MR imaging contrast effect, Fe_3O_4@CTAB, APTES-treated Fe_3O_4@SiO_2, Gd^{3+}-chelated Fe_3O_4@SiO_2, and commercial Resovist nanocontrast agents were evaluated in a 3T MRI system. The transverse relaxation rates ($1/T_2$) were evaluated, giving r_2 relaxivity coefficients of 97 $s^{-1}mM^{-1}$ (Fe_3O_4@CTAB), 211.8 $s^{-1}mM^{-1}$ (APTES-treated Fe_3O_4@SiO_2), 681 $s^{-1}mM^{-1}$(Gd^{3+}-chelated Fe_3O_4@SiO_2), and 91 $s^{-1}mM^{-1}$ (Resovist). Interestingly, the r_2 value increased 7-fold from Fe_3O_4@CTAB to Gd^{3+}-chelated Fe_3O_4@SiO_2. In contrast, the r_1 relaxivity was not apparently affected, giving ~0.9 and ~1.4 $s^{-1}mM^{-1}$ for Fe_3O_4@CTAB and Gd^{3+}-chelated Fe_3O_4@SiO_2, respectively. We introduced the BOLD sequence to acquire T_2* signals at different TEs, and calculated ΔR_2 and ΔR_2* mapping at the same time. Figure 2(a) shows the color ΔR_2* maps generated by the Gd^{3+}-chelated Fe_3O_4@SiO_2 nanoparticles; the regions of interest (ROIs) were placed in the liver parenchyma (outside of the vascular structure of the liver graft). The imaging contrast was immediately affected and darkened after 5 min. The signal in the liver quickly decreased to ~50% after 5 min, and then decayed to ~40% after 1h for Gd^{3+}-chelated Fe_3O_4@SiO_2 nanoparticles. We further tested Gd^{3+}-chelated Fe_3O_4@SiO_2 nanoparticles using a higher field with a 7T animal micro MRI system. The contrast signal of the lymph nodes (white arrows), liver (red arrows), spleen (blue arrows), and kidneys (orange arrows) were all reduced after Gd^{3+}-chelated Fe_3O_4@SiO_2 administration (Fig. 2(b)). The intensity of the lymph node, kidneys, and spleen dropped to 74%, 76%, and 49% after 1h, respectively, in T_2-weighted images (Fig. 2(c)). Detecting lymph-node metastasis is important during diagnosis, tumor staging, and subsequent clinical treatment. Iron oxide nanoparticles accumulate only in the normal nodes in the presence of macrophages. Gd^{3+}-chelated Fe_3O_4@SiO_2 nanoparticle images showed that the lymph node had a long-axis diameter of 2.6 mm and a short-axis diameter of 1.3 mm, which suggested that it was potent for detecting metastatic lymph nodes using Fe_3O_4/Gd nanocomposites.[1]

Beamlines 23A1 and 01C2 SWAXS and PXRD end stations

Reference

1. C.-C. Huang, C.-Y. Tsai, H.-S. Sheu, K.-Y. Chuang, C.-H. Su, U. Jeng, F.-Y. Cheng, C.-H. Su, H.-Y. Lei, and C.-S. Yeh, ACS Nano **5**, 3905 (2011).

Contact E-mail

csyeh@mail.ncku.edu.tw

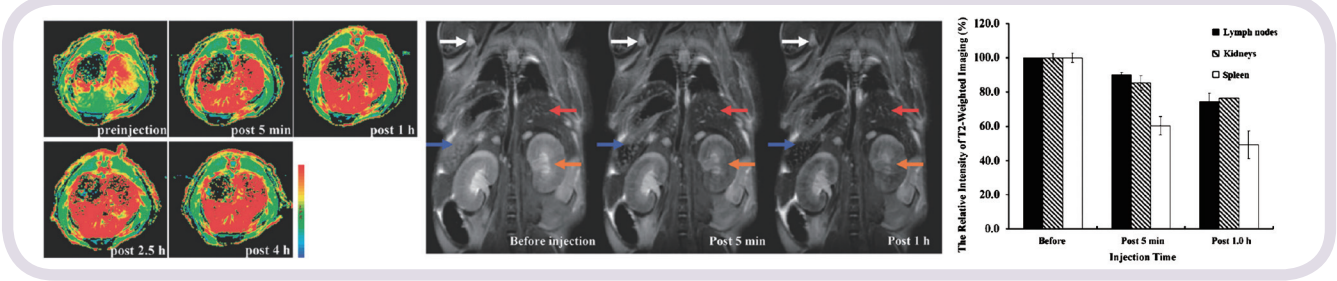

Fig. 2: Gd^{3+}-chelated Fe_3O_4@SiO_2 nanoparticles with which rats and mice had been treated (dose: 0.5 mg [Fe]/kg). (a) Color R_2* mapping of a rat liver at five time points using a clinical 3T scanner. (b) In vivo micro-T_2-weighted imaging of mice at three time points (white arrows, lymph node; red arrows, liver; blue arrows, spleen; and orange arrows, kidneys) using a 7T animal micro-MRI system. (c) Signal intensities in lymph nodes, kidneys, and spleen at the three time points.